



EFFECTS OF MgO WT.% ON THE STRUCTURE, MECHANICAL, AND BIOLOGICAL PROPERTIES OF BIOACTIVE GLASS-CERAMICS IN THE SiO₂, Na₂O, CaO, P₂O₅, MgO SYSTEM

Batool Abd Aladel, Israa K.Sabree, Shaker J. Edrees

Faculty of Materials Engineering, The University of Babylon, Iraq

ABSTRACT

Bioactive glass-ceramics used as a replacement material for bone tissues because of its bioactivity, compatibility, and abilities to form a crystallized hydroxyapatite (HA) bonding layer which has a similarity in composition and structure to the inorganic component of bones mineral phase. The major objectives of this research is estimating the effects of using MgO as an additive on the property of bioactive glass ceramic in 45SiO₂, 24.5 Na₂O, 6 P₂O₅, (24.5-x)CaO, X MgO where X= 0,1,3 and 5 wt.%. Bioactive glass ceramic was made by traditional glasses melting techniques at 1200°C for 2hr. Compressed sample sintered at (850)°C, the X-ray diffraction test confirmed the formations of (Na₂CaSi₃O₈) and (Na₂Ca₂Si₃O₉) phases in the structure of pure bioglass-ceramic and with (1wt.%) MgO, while (Na₂CaSiO₄) and CaMg(SiO₃)₂ phases were present in the structure of bioglass-ceramic with (3wt.%)MgO, and CaMg(SiO₃)₂ phase in the structure of bioglass-ceramic with (5wt.%) MgO. Results of mechanical and physical studies showed that increasing (MgO wt.%) in glass structure led to improving the bending strength, compressive strength, microhardness, and density associating with decreasing in porosity. FTIR confirmed the formations of the Si-O-Mg bond. The biological test was done by immersion the sample in (SBF) simulated body fluid for (21 days). XRD, SEM and pH tests revealed that appetite layers made on the samples surface, giving an evidence of their bioactivity. As general the results of the present study demonstrate that partial replacements of CaO by MgO in 45S5 glass ceramic improve the mechanical properties without altering the bioactivity suggesting that glass ceramic was suitable for the biomedical applications

Key words: MgO, bioglass-ceramics, Combite, bioactivity, melt-derived glass.

Cite this Article: Batool Abd Aladel, Israa K.Sabree, Shaker J. Edrees, Effects of MgO Wt.% on the Structure, Mechanical and Biological Properties of Bioactive Glass-Ceramics in the SiO₂, Na₂O, CaO, P₂O₅, MgO System, *International Journal of Mechanical Engineering and Technology* 10(1), 2019, pp. 97–106.

<http://www.iaeme.com/IJMET/issues.asp?JType=IJMET&VType=10&IType=1>

1. INTRODUCTION

Hench and their co-workers were largely responsible for the development of bioactive glasses which was known as 45S5 Bioglass[1]. Glasses and glass-ceramics are biocompatible and bioactive materials that could directly be attached to bones tissues by biological active hydroxyapatites (HA) layers that provide interfacial bonding. Such layers are structurally and chemically equivalent to the mineral phases of bones [2]. Unluckily, the low firmness of bioactive glass has restricted its uses to load bearing application [3]. It was proved that the mechanical property of bioglasses is managed by the addition of oxides like alumina, magnesia, titania, or zirconia [4] as well as by crystallization of bioactive glasses to produce glass-ceramic[5] Some glass ceramic in the CaO-SiO₂-P₂O₅-Na₂O systems with different phases, could be made by sintering and subsequent crystallization of powder of glasses showed excellent mechanical property and abilities for forming chemical a bond with living bones. Bioactive glass ceramic, group of osteoconductive biomaterial, is predestined material for a medical application, especially in orthopedic and dental implant, because of their food bioactivities and proven biocompatibility [6]. Generally, they made hydroxyapatite layers when simulated in solutions of buffered salt representing the ions concentrations of the fluids of the bodies (SBF or simulated body fluids)[7].

(Mg) Magnesium is the major intracellular earth metals cation being important elements in the bodies of humans [8], it is arranged as the fourth of plentiful cation in the bodies of humans especially in bones tissues (about 0.5% in bones or teeth enamels and more than 1% in teeth dentins)[9]

In the current study, bioglass-ceramic powder with the composition 45SiO₂, 24.5 Na₂O, 6 P₂O₅, (24.5-x)CaO, X MgO where X= 0,1,3 and 5 wt%.was prepared by melting derived technique followed by studying the change in the structure, physical and mechanical properties.

2. MATERIALS AND METHODS

Sodium Carbonate (Na₂CO₃, 98%, India), Silica foam (SiO₂, 99.9%, India), ((MgCO₃)Mg(OH)₂.5H₂O, India), phosphorus pentoxide (P₂O₅, 98%, China), and Calcium oxide (CaO) was synthesis from oyster shells.

2.1. Glass-ceramic preparation

45S5 bioactive glass that composed of 45wt% SiO₂, 24.5wt% Na₂O, 6 wt% P₂O₅, CaO(24.5-X)and X wt% MgO, where X=0,1,3 and 5 were prepared by conventional melting technique. For each type of bioactive glass, a 10 g of a batch is obtained by mixing an analytical reagent using planetary balls mills (SFM-1, QM-3SP2) run at 300 rpm, for 6 hour. The mixture was then melted in the alumina crucible at 1200 ± 10 °C for 2 hours in an electric furnace to guarantee complete melting, then the molten is permitted to cool gradually inside the oven. The obtained glass-ceramic is crushed by using mortar to get the semi-finished powder then milled by the planetary balls mills (SFM-1, QM-3SP2) keeps running at 300 rpm, for 12 hours. Table1 summarizes the composition of each prepared batch. Compacted samples with 10mm diameter and 30 mm were sintered at (1200) °C using 5 °C/min as heating rate.

Powders samples were analyst utilizing X-rays diffraction (Shimadzo, 6000) at rooms temperatures with CuK α radiations ($\lambda = 1.5405 \text{ \AA}$), and scanning speeds of 5°/min from 10° to 80° of 2 θ (Bragg angles) and 40 KV/30 mA applied powers for defining the structure and phase. The XRD peaks match with the standard JCPDS file (NO. 00-022-1455) for sodium calcium silicate (Na₂Ca₂Si₃O₉), (NO. 00-012-0671) for sodium calcium silicate (Na₂CaSi₃O₈), (NO. 00-024-1069) for sodium calcium silicate (Na₂CaSiO₄), and (NO.00-017-0318) for (CaMg(SiO₃)₂).

Table 1 The composition of each prepared sample

Code of the prepared glass powders	Composition (wt %)				
	SiO ₂	Na ₂ O	CaO	P ₂ O ₅	MgO
B0	45	24.5	24.5	6	0
B1	45	24.5	23.5	6	1
B3	45	24.5	21.5	6	3
B5	45	24.5	19.5	6	5

FTIR used to confirm the presence of MgO in the glass-ceramic structure. Apparent Porosity for the specimens was tested by Archimedes method using ASTM C373-88 (1988). Compressive strength was evaluated according to ASTM standard C-773-88(1999). Vickers Microhardness was measured according to ASTM C 1327-99, indentation load of 9.8 N, by the following equation.

$$H_v = 1.854(p/d^2) \quad (1)$$

H_v: Vickers hardness (Mpa), p: Loads (N), D: Diagonal lengths of the indentations impressions (μm).

Bending test was made according to ASTM C1161 procedure using a computerized universal testing appliance with tests of speed of 0.5 mm/min. the equations below were used to calculate the three-point bending strength.

$$\sigma_b = 3 p_f L / 2wt^2 \quad (2)$$

Where: σ_b: Bending strengths (MPa), P_f: Fractures loads (N), w: Samples width (mm), t: Samples thickness(mm).

In order to investigate samples bioactivity, (SBF) the simulated body fluid was prepared according to [10]. The sample was submerged in SBF at 37 °C for 21 days. EDS analysis was carried out for samples surfaces at the end of immersion time to check HA formation on the surfaces of immersion samples. pH of SBF solution was checked every day to observe the variation of (Ca and P) ion concentration in the solutions during immersion time.

2. RESULTS AND DISCUSSION

2.1. X-Rays Diffractions (XRD) Analysis

Figure1 showed the XRD analysis of prepared glass powders. (Na₂CaSi₃O₈) phase is found in the structure of (B0) and (B1) powders associated with decreasing in the crystallization rate for (B2), where the intensity of picks is changed significantly, while amorphous and no diffraction peaks in the XRD patterns were observed for (B3) and (B5) powders. This might be related to the abilities of MgO for increasing the viscosities of 45S5 glass by lessening the non-bridging oxygen in the glasses, so the rates of diffusions and mobility of the ion raised during crystallization processes [11].

For compact bioglass-ceramic samples sintered at 850 °C. Figure2 illustrates the XRD results. Two types of sodium calcium phosphate appears in (B0) and (B1) that are combeite (Na₂Ca₂Si₃O₉) that agrees with (JCPDS, card NO. 22-1455), in addition to the phase (Na₂CaSi₃O₈), which is common to the combeite in some peaks, this agrees with the results of many researchers [12][13][14].

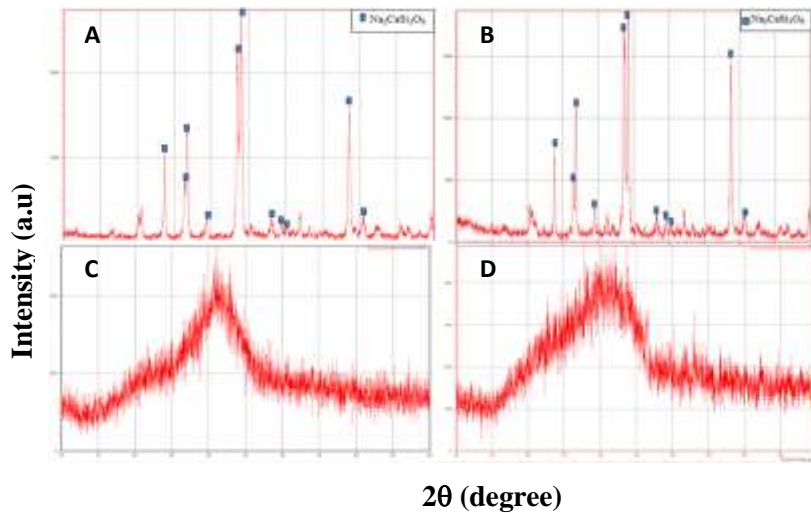


Figure 1 XRD pattern of (A): B0, (B): B1, (C): B3, (D): B5 of powders melted at 1200 °C.

This phase considers a bioceramic having a good bioactivity when immersed in a simulated body fluid, also shows better degradation resistance in the aqueous environment when compared to the amorphous bioglass[15]. $\text{Na}_2\text{CaSiO}_4$ and $\text{CaMg}(\text{SiO}_3)_2$ phases were present in (B3) while $\text{CaMg}(\text{SiO}_3)_2$ phase present in (B5). The last phase has potential candidates as Mg- and Si contains sources for bioceramic because it has found to be biocompatible, non- cytotoxic, and bioactive in vivo and in vitro. Elseways, dense diopside ceramic shows higher mechanical strengths and firmness, when compared to other bioceramic phase [16]. These agree with the results of many researchers [16][17].

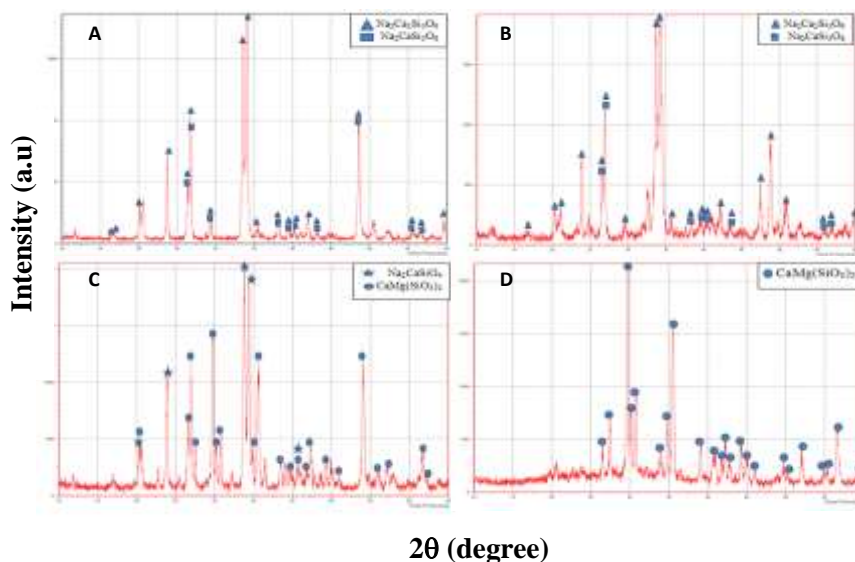


Figure 2 of (A): XRD pattern of (A): B0, (B): B1, (C): B3, (D): B5 compact bioglass-ceramic samples sintered at 850 °C

2.2. Results of FTIR Analysis

The improvement in mechanical properties of bioglass-ceramic samples may be attributed to the formation of Mg-O-Si bond as confirmed by FTIR results in Figure 3. Because magnesium ions were occupied interstitial sites within the bioglass-ceramic network.

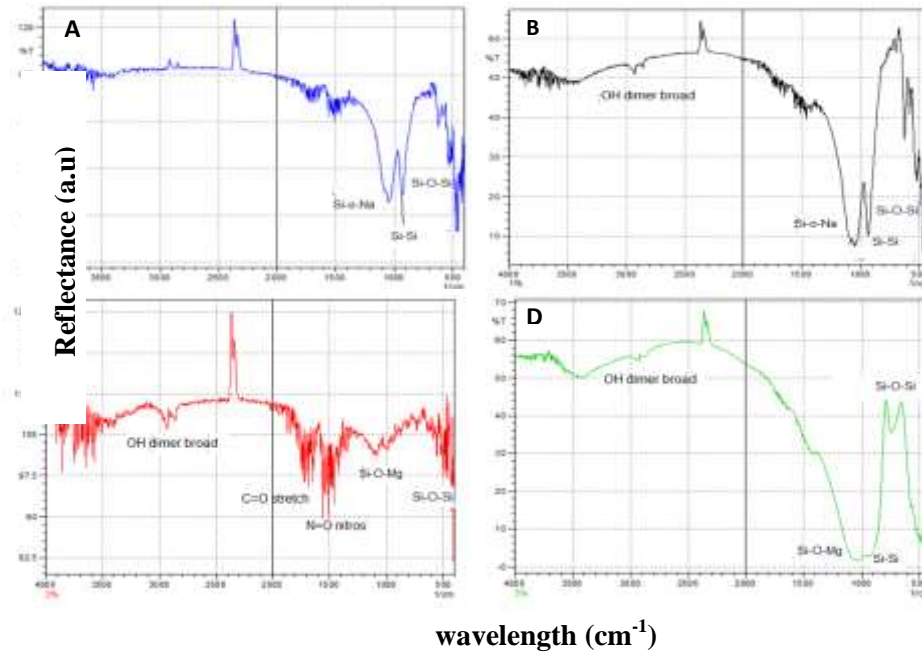


Figure 3 FTIR spectra of (A): B0, (B): B1, (C): B3, (D): B5 compact bioglass-ceramic samples sintered at 850 °C

2.3. SEM Analyses of Bioactive Glass-ceramic Sample

Figure 4 and 5 shows the images of (B0) and (B5) (sintered at 850 °C) respectively. Images (A) represent the scanning of the horizontal surface, while (B) represent the vertical broken surface of the samples. Obvious differences in the porosity are found in the morphology with different addition of MgO content in (B5) and without adding (MgO%) content in (B0). As illustrated in Figure 6, there was a decrease in porosity as the MgO% increase due to that the (MgO%) leads to high densification and exhibits the grain growth during sintering at 850 °C and the pores in (B0) are interconnected and distributed over a wide range.

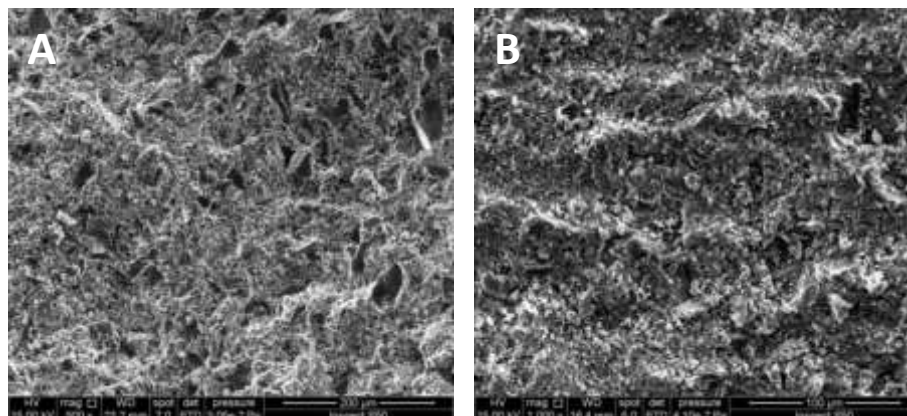


Figure 4: SEM images of (B0) samples. (A): Images of the surface of sample (B): Image of the fracture surface of samples

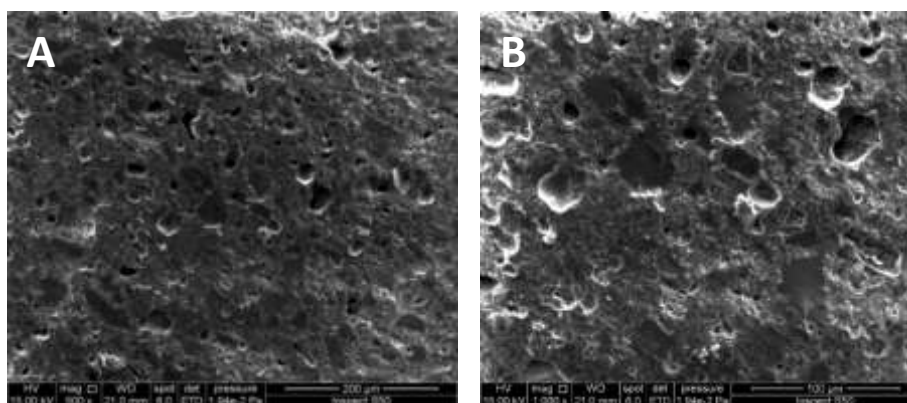


Figure 5: SEM images of (B5) samples. (A): Images of the surface of sample(B): Image of the fracture surface of samples

2.4. Density and Mechanical Properties Measurement

Figure 6 shows the bulk density and apparent porosity of the prepared bioglass-ceramic samples as a function of MgO weight percent. It can be observed that increasing MgO wt.% in the glass-ceramic leads to an increase in density from (1.17 to 2.58) gm/cm³ because of replacement a lighter element Ca (density = 1.55 g/cm³) by a heavier element, Mg (density = 3.58 g/cm³). Another reason considering the structural changes that take place, it was mentioned that the addition of modifying metal oxides (MgO) coordinated the NBOs (Mg-O-Si) and formed an interlink between the atoms, resulting in an increase in network connectivity and dimensionality. resulting in efficient compactness and packing in the bioglass-ceramic structure. The increase in density is ascribed to the reduction in average interatomic spacing in the bioglass-ceramic during the sintering [18] and this leads to a decrease in porosity from (30-5)%.

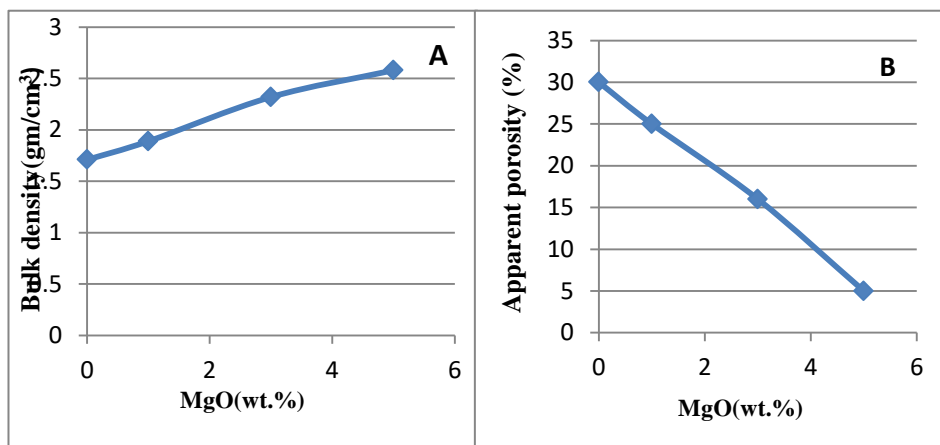


Figure 6 (A): Bulk density, (B): Apparent porosity of the sintered bioglass-ceramic samples as a function of MgO weight percent

Figure 7 illustrates that increasing MgO content from 1 to 5 wt% lead to a significant increase in the compressive strength, bending strength, and micro Vickers hardness. This attributed to the formations of a new strong bonds Mg-O-Si bond as proved in FTIR result. Magnesium ions were taken interstitial site within the bioglass-ceramic networks which lead to improving the density and mechanical property of the bioglass-ceramic samples and reinforcement of glass-ceramic structure. Also, the presence of CaMg(SiO₃)₂ phase in the structure as established by XRD may consider another reason for improving the mechanical properties because the new phase has high mechanical strength and toughness[16].

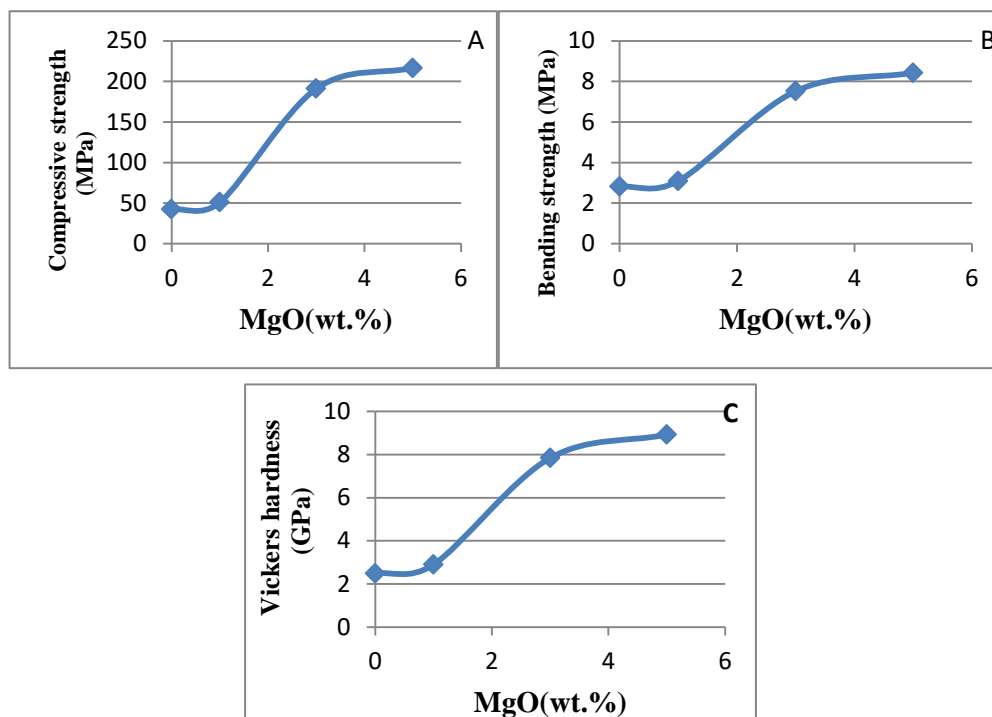
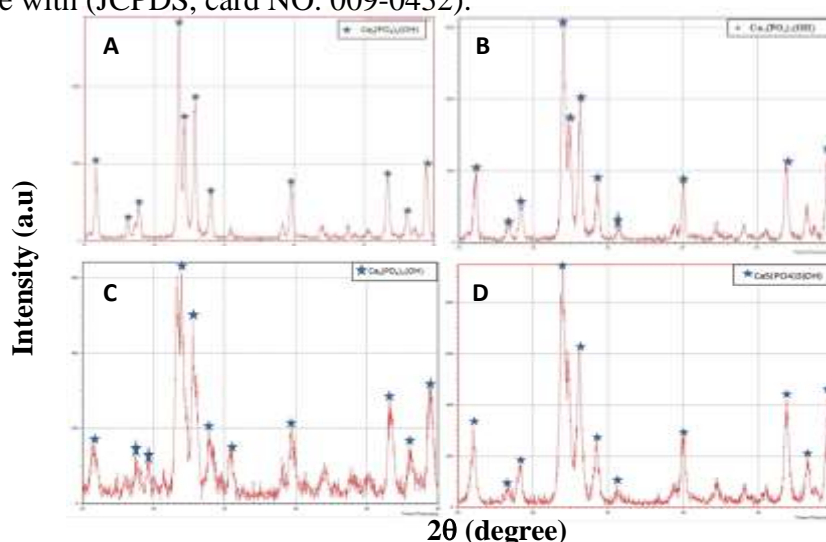


Figure 7 (A): Compressive, (B): Bending strength, (C): Vickers hardness of the sintered bioglass-ceramic samples as a function of MgO wt.%

2.5. In Vitro Bioactivity Tests

X-Rays diffractions analyses of bioactive glass sample:

It is a popular fact that the glass abilities for forming hydroxyapatite layers on the surfaces of the sample after immersions in an SBF are indications of its bioactivities and integrations with bones tissues [10]. XRD patterns in Figures 8 confirm a precipitation of hydroxyapatite (HA) on the surfaces after immersions in the SBF for all sintered samples with absence the phases present in Figure 2, proving that all surfaces were covered by HA layer and the partial substitutions of CaO by MgO not effect on glass-ceramic bioactivity. The crystalline peaks of (HA) agree with (JCPDS, card NO. 009-0432).



Figures 8: XRD pattern of (A): B0, (B): B1, (C): B3, (D): B5 compact bioglass-ceramic sample after immersions in SBF for 21 day

2.6. SEM Results of Bioglass-ceramic after Immersing in SBF Solutions

Obvious changes were noticed on the bioglass-ceramic sample after 21 days soaking in SBF as shown in Figure 9. An agglomerated of HA can be seen on the surface of (B0) and (B5) samples, which agree with the results of [19].

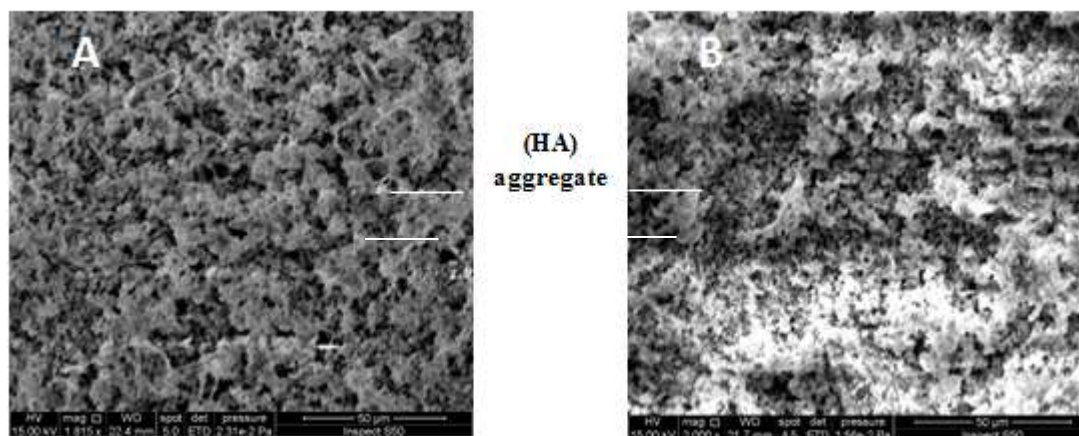


Figure 9: SEM images of (A): B0, (B): B5 sample after drenching in SBF for 21 day

2.6. pH Measurements

Figures 10 show the pH variation of SBF during immersing of bioactive glass-ceramic samples for 21 days. It reveals that for all bioactive samples of glasses, the pH rises within 1 to 7 day when compared to the first pH of the SBF solutions at 7.4. The rise in pH value is because of the fast release of Na^+ and Ca^{++} ion via exchanging with H^+ or H_3O^+ ion into the (SBF) solutions. The H^+ ion is replaced by cation that results in increasing in hydroxyl concentrations of the solutions, followed by breaking the silica glasses networks [14], that causes in the formations of silanols leading to low pH after the 7 days until the 21st day. The general behavior is similar to other researches that used bioactive glass with different

Composition [20]. The increase in pH indicates the formations of appetite layers on the surfaces of the of bioglass-ceramic as confirmed by the results of XRD and SEM image. We further note that increasing MgO wt% in glass-ceramic structure lead to decrease in solubility and the change of pH solution for (B1), (B3), and(B4) comparing with (B0) which attributed to Mg-O the chemical bond is stronger than Ca–O [21-23].

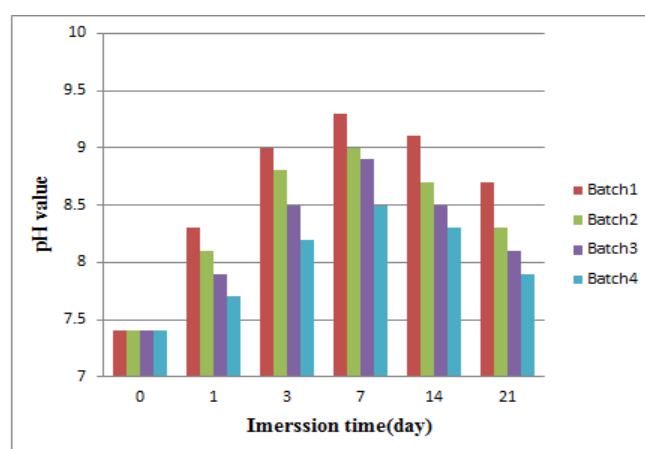


Figure 10: Variations of pH of the SBF solutions having bio glass-ceramic sample at a different time interval

3. CONCLUSIONS

The presence of different weight percent of MgO as network modifier oxide into the 45S5 bioactive glass-ceramic strongly influenced the resulting structure and mechanical properties. The structure changed depending on MgO wt.%; after sintering at 850°C, XRD results displayed existent of Combeite (Na₂CaSi₃O₈) phase in a glass-ceramic with 1wt.%MgO, while Diopside CaMg(SiO₃)₂ phase appeared in the structure of glass-ceramic with 3,5wt.% MgO. Although the two phases are biocompatible and bioactive but dense Diopside CaMg(SiO₃)₂ ceramics showed high mechanical strength, as compared to other bioceramic phases, resulting in significant increase in the material strength and hardness as well as increasing in bulk density with a reduction in porosity.

All of the prepared samples with (0,1,3,5)wt.%MgO formed apatite layers on their surfaces after immersions in SBF for 21 days, giving an evidence of their bioactivity. As general the result of this work demonstrate that the additions of (1,3,5)wt.% MgO to 45S5 glass-ceramic improve the mechanical properties without altering the bioactivity.

REFERENCES

- [1] Brink, M., Turunen, T., Happonen, R. P., & Yli-Urpo, A. (1997). Compositional dependence of bioactivity of glasses in the system Na₂O-K₂O-MgO-CaO-B₂O₃-P₂O₅-SiO₂. *Journal of Biomedical Materials Research: An Official Journal of The Society for Biomaterials and The Japanese Society for Biomaterials*, 37(1), 114-121.
- [2] De Aza, P. N., De Aza, A. H., Pena, P., & De Aza, S. (2007). Bioactive glasses and glass-ceramics. *Boletin-Sociedad Espanola De Ceramica Y Vidrio*, 46(2), 45.
- [3] Thompson, I. D., & Hench, L. L. (1998). Mechanical properties of bioactive glasses, glass-ceramics, and composites. *Proceedings of the Institution of Mechanical Engineers, Part H: Journal of Engineering in Medicine*, 212(2), 127-136.
- [4] Shackelford, J.F., 1999, "Bioceramics". Gordon and Breach Science Publishers imprint. vol 1.
- [5] El-Ghannam, A., Hamazawy, E., & Yehia, A. (2001). Effect of thermal treatment on bioactive glass microstructure, corrosion behavior, ζ potential, and protein adsorption. *Journal of biomedical materials research*, 55(3), 387-395.
- [6] Hoppe, A., Güldal, N. S., & Boccaccini, A. R. (2011). A review of the biological response to ionic dissolution products from bioactive glasses and glass-ceramics. *Biomaterials*, 32(11), 2757-2774.
- [7] Huygh, A., Schepers, E. J. G., Barbier, L., & Ducheyne, P. (2002). Microchemical transformation of bioactive glass particles of narrow size range, a 0–24 months study. *Journal of Materials Science: Materials in Medicine*, 13(3), 315-320.
- [8] Saris, N. E. L., Mervaala, E., Karppanen, H., Khawaja, J. A., & Lewenstam, A. (2000). Magnesium: an update on physiological, clinical and analytical aspects. *Clinica chimica acta*, 294(1-2), 1-26.
- [9] Staiger, M. P., Pietak, A. M., Huadmai, J., & Dias, G. (2006). Magnesium and its alloys as orthopedic biomaterials: a review. *Biomaterials*, 27(9), 1728-1734.
- [10] Kokubo, T., Kushitani, H., Sakka, S., Kitsugi, T., & Yamamuro, T. (1990). Solutions able to reproduce in vivo surface-structure changes in bioactive glass-ceramic A-W3. *Journal of biomedical materials research*, 24(6), 721-734.

- [11] Hashmi, M. U., Shah, S. A., Zaidi, M. J., & Alam, S. (2012). Effect of different CaO/MgO ratios on the structural and mechanical properties of bioactive glass-ceramics. *Ceramics-Silikáty*, 56(4), 347-351.
- [12] Brentrup, G. J., Moawad, H. M., Santos, L. F., Almeida, R. M., & Jain, H. (2009). Structure of Na₂O–CaO–P₂O₅–SiO₂ glass–ceramics with multimodal porosity. *Journal of the American Ceramic Society*, 92(1), 249-252.
- [13] Adrees, A. P. D. S. J., & Abdalwahad, M. S. R. I., (2017), Preparation of Hydroxyapatite and Bioactive Glass Ceramic to Get Biocomposite by Using a Genetic Algorithm Method, IEEE First International Conference on Recent Trends of Engineering Science and Sustainability.
- [14] Eraba, K. M. T., Hassan, M. Y., Hamazawy, E., Hadad, A., & Ayoub, H. A. (2015), Characterization of bioglass ceramic after addition of fluorine in Na₂O–CaO–SiO₂ system.
- [15] Plewinski, M., Schickle, K., Lindner, M., Kirsten, A., Weber, M., & Fischer, H. (2013). The effect of crystallization of bioactive bioglass 45S5 on apatite formation and degradation. *Dental Materials*, 29(12), 1256-1264.
- [16] García Carrodeguas, R., Córdoba, E., De Aza, A. H., De Aza, S., & Pena, P. (2009). Bone-Like Apatite-Forming Ability of Ca₃ (PO₄)₂-CaMg (SiO₃)₂ Ceramics in Simulated Body Fluid. In *Key Engineering Materials* (Vol. 396, pp. 103-106). Trans Tech Publications.
- [17] Sainz, M. A., Pena, P., Serena, S., & Caballero, A. (2010). Influence of design on bioactivity of novel CaSiO₃–CaMg (SiO₃)₂ bioceramics: In vitro simulated body fluid test and thermodynamic simulation. *Acta Biomaterialia*, 6(7), 2797-2807.
- [18] Newby, P.J; El-Gendy ,R.; Kirkham, J.; Yang, X.B.;Thompson, I.D.; and Boccaccini AR., (2011), " Ag-doped 45S5 Bioglass®-based bone scaffolds by molten salt ion exchange: processing and characterisation". *J Mater Sci Mater Med*.22(3):557–69.
- [19] Souza, M. T., Crovace, M. C., Schröder, C., Eckert, H., Peitl, O., & Zanotto, E. D. (2013). Effect of magnesium ion incorporation on the thermal stability, dissolution behavior and bioactivity in Bioglass-derived glasses. *Journal of Non-Crystalline Solids*, 382, 57-65.
- [20] Mahdi, O. S., & Sabri, I. Q. (2016). Characterization, Mechanical, and In Vitro Bioactivity Properties of Hydroxyapatite/Bioactive Glass Composite. *Journal of University of Babylon*, 24(4), 820-831.
- [21] Souza, M. T., Crovace, M. C., Schröder, C., Eckert, H., Peitl, O., & Zanotto, E. D. (2013). Effect of magnesium ion incorporation on the thermal stability, dissolution behavior and bioactivity in Bioglass-derived glasses. *Journal of Non-Crystalline Solids*, 382, 57-65.
- [22] Kadhim Naief Kadhim and Ahmed H. (Experimental Study Of Magnetization Effect On Ground Water Properties).*Jordan Journal of Civil Engineering*, Volume 12, No. 2, 2018
- [23] Jha, P., & Singh, K. (2016). Effect of MgO on bioactivity, hardness, structural and optical properties of SiO₂–K₂O–CaO–MgO glasses. *Ceramics International*, 42(1), 436-444.